ACS Catalysis

Letter

pubs.acs.org/acscatalysis

Selective Propene Oligomerization with Nickel(II)-Based Metal–Organic Frameworks

Anton N. Mlinar,[†,§] Benjamin K. Keitz,[‡,§] David Gygi,[‡] Eric D. Bloch,[‡] Jeffrey R. Long,*[,‡] and Alexis T. Bell*[,†]

[†]Department of Chemical and Biomolecular Engineering, [‡]Department of Chemistry, University of California, Berkeley, Berkeley, California 94720-1462, United States

Supporting Information

ABSTRACT: Two Ni^{2+}-containing metal–organic frameworks, Ni_2(dobdc) and Ni_2(dobpdc), are shown to be active for the oligomerization of propene in the gas phase. The metal–organic frameworks exhibit activity comparable to Ni^{2+}-exchanged aluminosilicates but maintain high selectivity for linear oligomers. Thus, these frameworks should enable the high yielding synthesis of linear propene oligomers for use in detergent and diesel fuel applications.

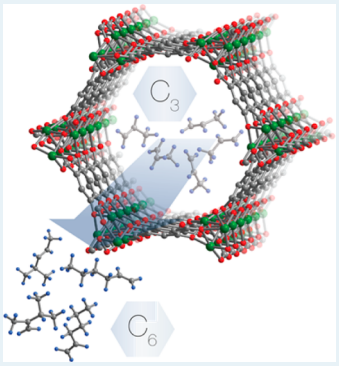

KEYWORDS: *metal–organic frameworks, catalysis, oligomerization, propene, nickel*

Heterogeneous nickel aluminosilicate materials have been demonstrated to be active and selective catalysts for light olefin oligomerization,[1−3] offering a means of producing liquid transportation fuels and detergents from light hydrocarbon gases. Recent work has shown that catalytic activity arises from isolation of Ni^{2+} cations on the support[4,5] and that stable gas-phase propene oligomerization activity can be achieved with Ni^{2+}-exchanged Na–X zeolites at low nickel loadings.[5] Exchange of the Na^+ cations for alkali metal and alkaline earth cations in Ni–Na–X was found to alter the free volume in the zeolite supercage, leading to increased catalyst activity and dimer branching for catalysts with the most open space in the zeolite supercage.[6] Specifically, Ni–Sr–X, the catalyst with the largest supercage free volume, exhibited the highest rate of dimer formation per Ni, 52 h^{-1}, and the highest degree of dimer branching, 70%, at 453 K and 5 bar of propene pressure. In contrast, Ni–K–X, the catalyst with the smallest open volume, limited the degree of dimer branching to 36%, but also decreased the dimer formation rate per Ni to 7 h^{-1} under the same conditions. Further increasing the space around the Ni^{2+} sites by using larger mesoporous aluminosilicate materials led to higher catalytic activity under the same reaction conditions but diminished control over dimer branching, with all catalysts exhibiting ∼49% branched products.[7] These results suggest that although pore space near the Ni^{2+} site governs catalytic activity, close steric and electronic control of the site influences the degree of oligomer branching. Thus, there appears to be a trade-off in these materials between catalytic activity and the production of linear products because the strong interactions between the site and support required to produce linear oligomers can be achieved only by decreasing the pore size, which necessarily limits catalytic activity. As a consequence, there is a need to develop catalytic materials that combine high activity with good selectivity for linear oligomers to produce high yields of molecules more suitable as diesel fuel and detergents.

Metal–organic frameworks are a relatively new class of porous materials consisting of crystalline arrays of metal cations connected in three dimensions by multitopic organic linkers.[8,9] A select subset of such materials contain coordinatively unsaturated metal centers that can serve as adsorption sites for small molecules and act as Lewis acids.[10−14] The predictable location of these open metal sites, combined with the tunability of the organic linker, has positioned metal–organic frameworks as potential alternatives to zeolites in a variety of catalysis applications;[15−17] however, examples of metal–organic framework catalysts that are competitive with zeolites, particularly in gas-phase reactions, are rare.[18]

Here, we show that Ni_2(dobdc) ($dobdc^{4-}$ = 2,5-dioxodo-1,4-benzenedicarboxylate; Ni-MOF-74)[19] and Ni_2(dobpdc) ($dobpdc^{4-}$ = 4,4′-dioxodo-[1,1′-biphenyl]-3,3′-dicarboxylate), two metal–organic frameworks with high concentrations of coordinatively unsaturated Ni^{2+} sites, serve as gas-phase propene oligomerization catalysts. The location of the Ni^{2+}

Received: December 13, 2013
Revised: January 22, 2014
Published: January 27, 2014

cations within the framework allows for local steric and electronic control of the active sites, and the large pore sizes enable a high oligomerization activity. We note that our results validate recent spectroscopic and ethylene gas adsorption data suggesting Ni_2(dobdc) may act as an oligomerization catalyst and that our approach is conceptually different from recent reports using homogeneous Ni catalysts *supported* in metal–organic frameworks and other materials as liquid-phase olefin oligomerization catalysts.[20−24] As such, this work represents a rare example of metal–organic framework-based catalysis in which the metal nodes exhibit catalytic activity in a gas phase reaction.[18] Finally, we show that Ni_2(dobdc) and Ni_2(dobpdc) limit the degree of dimer branching while maintaining high catalytic activity, allowing for a higher yield of linear oligomers than currently observed with heterogeneous aluminosilicate propene oligomerization catalysts.

The isoreticular frameworks Ni_2(dobdc) and Ni_2(dobpdc) belong to the MOF-74 structure type[19,25,26] and are constructed of helical chains of Ni^{2+} atoms arranged in a honeycomb lattice of hexagonal, one-dimensional channels with diameters of 10.3 and 18.4 Å, respectively (Figure 1). Prior to activation, the coordination environment of each Ni^{2+} center can be described as distorted octahedral and is completed by a bound DMF molecule projecting into the framework channels. Solvent exchange with MeOH, followed by heating to 453 K under dynamic vacuum for ∼3 days generated the fully activated materials with square pyramidal Ni^{2+} featuring an open coordination site. The porosity of the resulting Ni_2(dobdc) and Ni_2(dobpdc) materials was confirmed by N_2 adsorption at 77 K, which yielded BET surface areas of 1160 and 2059 $m^2\ g^{-1}$, respectively.

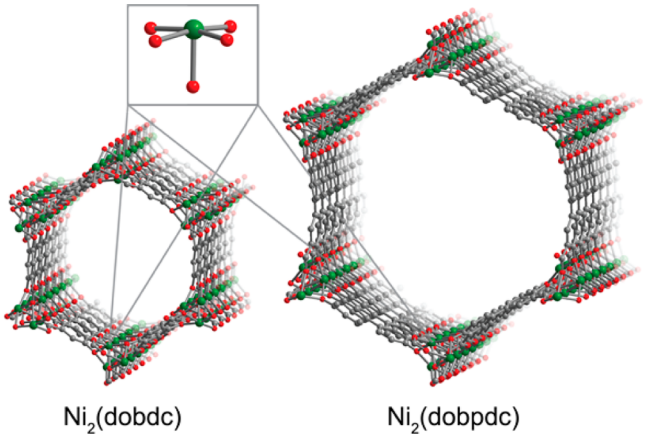

Figure 1. The framework structures of Ni_2(dobdc) and Ni_2(dobpdc) derived from single-crystal X-ray analysis of the isostructural solvated zinc framework, in the case of Ni_2(dobpdc).[19,26] Ni, C, and O atoms are depicted as green, gray, and red, respectively; H atoms are omitted for clarity. Inset: The coordination sphere of a single Ni^{2+} in Ni_2(dobdc) and Ni_2(dobpdc) following removal of the bound solvent molecule.

The catalytic activity of Ni_2(dobdc) and Ni_2(dobpdc) for propene oligomerization was examined at 453 K and 5 bar of propene pressure using a fixed bed reactor. The results of these time-on-stream experiments are presented in Figure 2. Both catalysts were determined to be >99% selective for oligomers during the entire course of the experiment. Propene dimers comprised >95% of the oligomeric product mixture, with the remainder being trimers (Supporting Information Table S1).

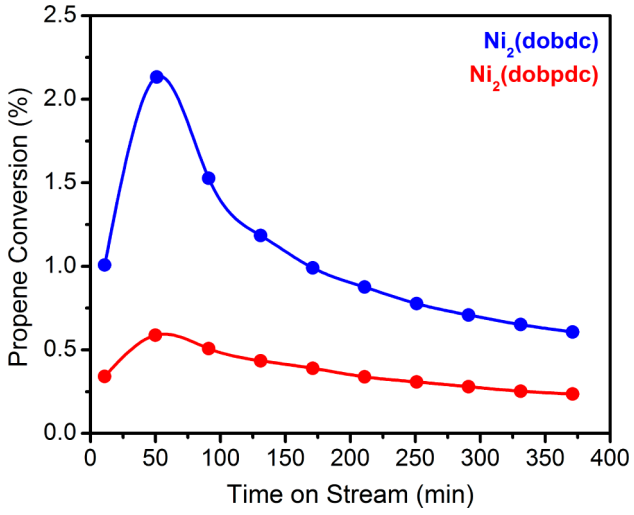

Figure 2. Time-on-stream propene oligomerization activity of Ni_2(dobdc) and Ni_2(dobpdc) at 453 K and 5 bar propene pressure. Flow rate ($C_3^=$) = 30 $cm^3\ min^{-1}$ STP, weight hour space velocity (WHSV) = 64 h^{-1}.

The metal–organic frameworks retained their crystallinity after the catalysis run, as confirmed by powder X-ray diffraction (Supporting Information Figure S4). A control experiment confirmed that the catalytic activity arose from the presence of Ni^{2+} cations because the isostructural metal–organic framework Mg_2(dobdc) was found to be completely inactive for propene oligomerization under identical reaction conditions. Similar to nickel aluminosilicate olefin oligomerization catalysts,[3,27] preliminary results suggest that the Ni^{2+}-containing metal–organic frameworks are also active for oligomerization of other olefins. Specifically, under the same reaction conditions, ethene was determined to be more reactive than propene (see Supporting Information Figure S1) and produced oligomers with >99.9% selectivity (>95% dimers). Along with the inactivity of Mg_2(dobdc), this further suggests that the observed activity arises from the Ni^{2+} sites and not from defect Brønsted acid sites, which are known to be less reactive toward ethene.[3]

As shown in Figure 2, the catalytic activity of both metal–organic frameworks initially increased with time on-stream before gradually deactivating. Because mechanisms for propene oligomerization require the use of more than one coordination site, we hypothesize that the activation of the catalysts is likely due to coordination of propene to a Ni^{2+} site, followed by displacement of at least one Ni–O ligand interaction to form the active Ni–alkyl site, similar to the active species proposed for homogeneous Ni-based catalysts[28] and Ni–X zeolites.[6] In partial support of this hypothesis, we note that the binding of propene to Ni^{2+} in Ni_2(dobdc) is quite strong, with an initial isosteric heat of adsorption of 53 kJ mol^{-1}, and that the prerequisite olefin complex has been structurally characterized by powder neutron diffraction for the isostructural metal–organic frameworks Co_2(dobdc) and Fe_2(dobdc).[21,29] However, at this time, we cannot rule out other potential activation mechanisms.

Comparison of the gas-phase propene oligomerization activity of Ni_2(dobdc), Ni–Na–X,[5] and Ni–Na–MCM-41[7] under the same conditions indicated that the activity of the two metal–organic frameworks was comparable to those of the Ni-

dx.doi.org/10.1021/cs401189a | ACS Catal. 2014, 4, 717−721

exchanged aluminosilicate materials when using the same weight of catalyst (Figure 3A).

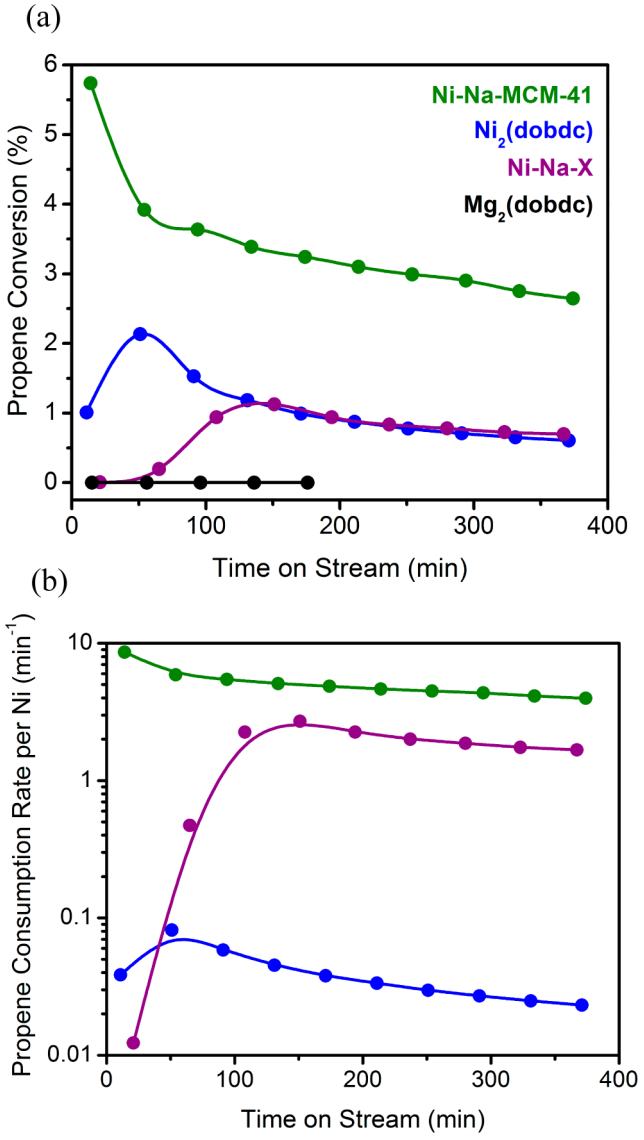

Figure 3. (a) Comparison of propene oligomerization activity of Ni_2(dobdc) (blue) to that of Ni−Na−X (purple),[5] Ni−Na−MCM-41 (green),[7] and Mg_2(dobdc) (black) at 453 K, 5 bar propene pressure, and WHSV = 64 h^{-1}. (b) Propene consumption rate per Ni^{2+} site (log scale) assuming 100% of Ni^{2+} in each material is active plotted as a function of time on-stream. T = 453 K, P = 5 bar $C_3^=$, WHSV = 64 h^{-1}.

However, because both Ni_2(dobdc) and Ni_2(dobpdc) contain a much higher weight loading of Ni than either Ni−Na−X or Ni−Na−MCM-41 (37.7 and 30.3 wt %, respectively, as compared with 0.6 wt %), this means that the metal−organic frameworks are significantly less active than the Ni-exchanged aluminosilicates on a per Ni basis (see Figure 3b). It is noted that the decrease could be due to either a lower intrinsic Ni^{2+} site activity or a lower percentage of sites being active for oligomerization in the framework structure. Close examination of Figure 2 shows that the deactivation rate of Ni_2(dobdc) was found to be similar to that of the Ni-exchanged aluminosilicate materials, indicating a common deactivation pathway. As has been postulated for Ni-exchanged aluminosilicates, this deactivation may be due to the accumulation of long oligomers in the pores. We attempted to find evidence for this deactivation pathway in the metal−organic frameworks but were unable to detect any higher molecular weight oligomers via NMR spectroscopy following dissolution of the frameworks in acidified DMSO-d_6. Nevertheless, the use of higher olefin pressures[2] or slurry reactors[30] has enabled nickel aluminosilicate catalysts to reach conversions of >98% while maintaining >98% selectivity to oligomers, suggesting that the similarly active Ni^{2+}-containing metal−organic frameworks examined here could reach equally high conversions with similar changes to the reaction system.

Importantly, although the activity of Ni_2(dobdc) and Ni_2(dobpdc) is similar to that of Ni−Na−X, the metal−organic frameworks exhibit an increased selectivity for forming linear propene dimers (Figure 4 and Supporting Information Table S2). The degree of dimer branching was not determined to be a function of the conversion or pore size, with Ni_2(dobdc) and Ni_2(dobpdc) producing ∼38% branched dimers at all times on stream. This agrees well with recent results using Ni-exchanged MCM-41 materials in which it was determined that the large pore space around the Ni sites causes little influence of pore size on the dimer isomer distribution.[7] The cause for the enhanced selectivity to linear oligomers in the metal−organic frameworks relative to the Ni-exchanged aluminosilicate materials is attributed to the incorporation of the active Ni^{2+} sites within the framework. The increased sterics around these sites likely promotes the formation of a terminal Ni−alkyl intermediate species, thereby enhancing linear dimer formation in a manner similar to that previously reported for Ni−X zeolites.[6] Combining the results presented in Figures 3 and 4 indicates that this increase in linear dimer selectivity does not come at the expense of catalytic activity, in contrast to what has been reported with alkali metal- and alkaline earth-exchanged Ni−X zeolites. This suggests that incorporation of Ni^{2+} into the unique coordination environment afforded by the framework results in a material capable of producing linear oligomers in

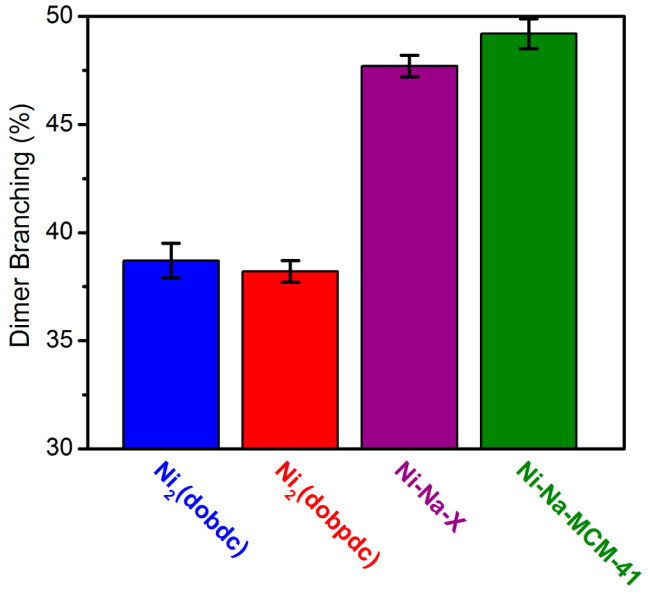

Figure 4. Degree of dimer branching for Ni_2(dobdc) and Ni_2(dobpdc) compared with that for Ni−Na−X and Ni−Na−MCM-41 at 400 min of time on stream, 453 K, 5 bar propene pressure, and WHSV = 64 h^{-1}.

dx.doi.org/10.1021/cs401189a | ACS Catal. 2014, 4, 717−721

higher yields than is possible with Ni-exchanged aluminosilicates.

In summary, we have shown that Ni_2(dobdc) and Ni_2(dobpdc), which contain wide one-dimensional channels lined with coordinatively unsaturated Ni^{2+} sites, are active catalysts for the oligomerization of propene in the gas phase. The metal−organic framework catalysts displayed catalytic activity comparable to that of Ni^{2+}-exchanged aluminosilicates, but exhibited increased selectivity for linear oligomerization products. Although there are many competitive processes for the oligomerization of ethene and propene, the described metal−organic frameworks offer a promising route for the production of linear products from olefins, allowing for the synthesis of molecules suitable as diesel fuel additives or detergent precursors using many different olefin feeds. Future efforts will be devoted to determining the nature of the catalytically active species and the origin of the high linear selectivity.

EXPERIMENTAL SECTION

Ni_2(dobdc) was prepared according to literature procedures.[19] For the synthesis of Ni_2(dobpdc), a 20-mL glass scintillation vial was charged with H_4dobpdc (41.1 mg, 0.150 mmol),[26] $Ni(NO_3)_2{\cdot}6H_2O$ (109 mg, 0.375 mmol), and 15 mL of mixed solvent (1:1:1 H_2O/DMF/EtOH). The vial was sealed with a Teflon-lined cap and placed in a 2-cm-deep well plate on a 393 K hot plate. After 36 h, a green powder formed on the bottom of the vial. The reaction mixture was then decanted, and the remaining powder was soaked in DMF at 343 K for 12 h, after which the solvent was decanted and replaced with fresh DMF. This process was repeated six times over the course of 3 days, after which the solvent was switched to methanol and the process repeated. The solid was then collected by filtration and fully desolvated by heating under dynamic vacuum (<10 μbar at 523 K for 72 h). The crystallinity of Ni_2(dobpdc) was confirmed by powder X-ray diffraction, and its surface area was measured by N_2 adsorption at 77 K (see Supporting Information for details).

The catalytic activity was measured using a 0.5-in. stainless steel reactor setup described elsewhere.[7] To make the fixed bed, 50 mg of activated Ni_2(dobdc) or Ni_2(dobpdc) was mixed with 450 mg of Silicycle silica (average pore diameter = 150 Å; surface area = 300 m^2 g^{-1}) in a glovebox and then rapidly transferred into the reactor to minimize exposure to the atmosphere. The sample was then pretreated overnight at 453 K under 100 cm^3 min^{-1} helium (Praxair, 99.999%) to remove water adsorbed during preparation of the reactor. Following pretreatment, the feed was switched to propene (Praxair, 99.9%), and the pressure was raised to 5 bar while maintaining the reactor temperature at 453 K. Products were analyzed using an Agilent 7890A gas chromatograph equipped with two gas-sampling valves, separation columns, and FID detectors as described previously.[7]

ASSOCIATED CONTENT

Supporting Information

Experimental details, materials characterization, and detailed hydrocarbon analysis. This material is available free of charge via the Internet at http://pubs.acs.org.

AUTHOR INFORMATION

Corresponding Authors

*E-mail: jrlong@berkeley.edu.

*E-mail: bell@cchem.berkeley.edu.

Author Contributions

§A.N.M. and B.K.K. contributed equally.

Notes

The authors declare no competing financial interest.

ACKNOWLEDGMENTS

We thank Otto Ho for help with carrying out the catalytic experiments and BP's XC^2 program for funding this study.

REFERENCES

(1) Heveling, J.; Van der Beek, A.; De Pender, M. *Appl. Catal.* **1988**, *42*, 325−336.

(2) Heveling, J.; Nicolaides, C. P.; Scurrell, M. S. *Appl. Catal., A* **1998**, *173*, 1−9.

(3) Corma, A.; Iborra, S. *Catalysts for Fine Chemical Synthesis*; Derouane, E. G., Ed.; J. Wiley & Sons Ltd.: United Kingdom, 2006; pp 125−132.

(4) Tanaka, M.; Itadani, A.; Kuroda, Y.; Iwamoto, M. *J. Phys. Chem. C* **2012**, *116*, 5664−5672.

(5) Mlinar, A. N.; Baur, G. B.; Bong, G. G.; Getsoian, A.; Bell, A. T. *J. Catal.* **2012**, *296*, 156−164.

(6) Mlinar, A. N.; Ho, O. C.; Bong, G. G.; Bell, A. T. *ChemCatChem* **2013**, *5*, 3139−3147.

(7) Mlinar, A. N.; Shylesh, S.; Ho, O. C.; Bell, A. T. *ACS Catal.* **2014**, *4*, 337−343.

(8) Tranchemontagne, D. J.; Mendoza-Cortés, J. L.; O'Keeffe, M.; Yaghi, O. M. *Chem. Soc. Rev.* **2009**, *38*, 1257−1283.

(9) Stock, N.; Biswas, S. *Chem. Rev.* **2012**, *112*, 933−969.

(10) Dincă, M.; Long, J. R. *Angew. Chem., Int. Ed.* **2008**, *47*, 6766−6779.

(11) Dincă, M.; Dailly, A.; Liu, Y.; Brown, C. M.; Neumann, D. A.; Long, J. R. *J. Am. Chem. Soc.* **2006**, *128*, 16876−16883.

(12) Zhou, W.; Wu, H.; Yildirim, T. *J. Am. Chem. Soc.* **2008**, *130*, 15268−15269.

(13) Chen, B.; Ockwig, N. W.; Millward, A. R.; Contreras, D. S.; Yaghi, O. M. *Angew. Chem., Int. Ed.* **2005**, *44*, 4745−4749.

(14) Rosi, N. L.; Kim, J.; Eddaoudi, M.; Chen, B.; O'Keeffe, M.; Yaghi, O. M. *J. Am. Chem. Soc.* **2005**, *127*, 1504−1518.

(15) Lee, J.; Farha, O. K.; Roberts, J.; Scheidt, K. A.; Nguyen, S. T.; Hupp, J. T. *Chem. Soc. Rev.* **2009**, *38*, 1450−1459.

(16) Farrusseng, D.; Aguado, S.; Pinel, C. *Angew. Chem., Int. Ed.* **2009**, *48*, 7502−7513.

(17) Yoon, M.; Srirambalaji, R.; Kim, K. *Chem. Rev.* **2012**, *112*, 1196−1231.

(18) Valvekens, P.; Vermoortele, F.; De Vos, D. *Catal. Sci. Technol.* **2013**, *3*, 1435−1445.

(19) Dietzel, P. D. C.; Panella, B.; Hirscher, M.; Blom, R.; Fjellvåg, H. *Chem. Commun.* **2006**, *1*, 959−961.

(20) Chavan, S.; Bonino, F.; Vitillo, J. G.; Groppo, E.; Lamberti, C.; Dietzel, P. D. C.; Zecchina, A.; Bordiga, S. *Phys. Chem. Chem. Phys.* **2009**, *11*, 9811−9822.

(21) Geier, S. J.; Mason, J. A.; Bloch, E. D.; Queen, W. L.; Hudson, M. R.; Brown, C. M.; Long, J. R. *Chem. Sci.* **2013**, *4*, 2054−2061.

(22) Canivet, J.; Aguado, S.; Schuurman, Y.; Farrusseng, D. *J. Am. Chem. Soc.* **2013**, *135*, 4195−4198.

(23) Kyogoku, K.; Yamada, C.; Suzuki, Y.; Nishiyama, S.; Fukumoto, K.; Yamamoto, H.; Sano, M.; Miyake, T. *J. Jpn. Pet. Inst.* **2010**, *53*, 308−312.

(24) Angelescu, E.; Che, M.; Andruh, M.; Zavoainu, R.; Costentin, G.; Mirica, C.; Pavel, O. D. *J. Mol. Catal. A: Chem.* **2004**, *219*, 13−19.

(25) Caskey, S. R.; Wong-Foy, A. G.; Matzger, A. J. *J. Am. Chem. Soc.* **2008**, *130*, 10870−10871.

(26) McDonald, T. M.; Lee, W. R.; Mason, J. A.; Wiers, B. M.; Hong, C. S.; Long, J. R. *J. Am. Chem. Soc.* **2012**, *134*, 7056−7065.

(27) Heveling, J.; Nicolaides, C. P.; Scorrell, M. S. *Catal. Lett.* **2004**, *95*, 87−91.

(28) Skupińska, J. *Chem. Rev.* **1991**, *91*, 613s−648.
(29) Bloch, E. D.; Queen, W. L.; Krishna, R.; Zadrozny, J. M.; Brown, C. M.; Long, J. R. *Science* **2012**, *335*, 1606−1610.
(30) Lallemand, M.; Finiels, A.; Fajula, F.; Hulea, V. *Chem. Eng. J.* **2011**, *172*, 1078−1082.